

Suppression of magnetic excitations near the surface of the topological Kondo insulator SmB_6

P. K. Biswas,^{1,2,*} M. Legner,³ G. Balakrishnan,⁴ M. Ciomaga Hatnean,⁴ M. R. Lees,⁴ D. McK. Paul,⁴ E. Pomjakushina,⁵ T. Prokscha,¹ A. Suter,¹ T. Neupert,⁶ and Z. Salman^{1,†}

¹Laboratory for Muon Spin Spectroscopy, Paul Scherrer Institut, CH-5232 Villigen PSI, Switzerland

²ISIS Pulsed Neutron and Muon Source, STFC Rutherford Appleton Laboratory, Harwell Campus, Didcot, Oxfordshire, OX11 0QX, United Kingdom

³Institut für Theoretische Physik, ETH Zürich, 8093 Zürich, Switzerland

⁴Department of Physics, University of Warwick, Coventry, CV4 7AL, UK

⁵Laboratory for Scientific Developments and Novel Materials, Paul Scherrer Institut, CH-5232 Villigen PSI, Switzerland

⁶Physik-Institut, Universität Zürich, Winterthurerstrasse 190, 8057 Zürich, Switzerland

We present a detailed investigation of the temperature and depth dependence of the magnetic properties of 3D topological Kondo insulator SmB_6 , in particular near its surface. We find that local magnetic field fluctuations detected in the bulk are suppressed rapidly with decreasing depths, disappearing almost completely at the surface. We attribute the magnetic excitations to spin excitons in bulk SmB_6 , which produce local magnetic fields of about ~ 1.8 mT fluctuating on a time scale of ~ 60 ns. We find that the excitonic fluctuations are suppressed when approaching the surface on a length scale of 40–90 nm, accompanied by a small enhancement in static magnetic fields. We associate this length scale to the size of the excitonic state.

PACS numbers: 71.27.+a, 74.25.Jb, 75.70.-i, 76.75.+i

Introduction — Topological Insulators (TIs) are a class of quantum materials that are characterized by a fully insulating gap in the bulk and robust metallic topological surface states. It was suggested that these are promising materials for electronic spin manipulation [1]. Theoretical studies predicted that the prototypical Kondo insulator SmB_6 belongs to this new class of materials [2–5]. This was later supported by transport [6–9] and angle-resolved photoemission spectroscopy (ARPES) [10–12] measurements. Xu *et al.* have also revealed that the surface states of SmB_6 are spin polarized [13], where the spin is locked to the crystal momentum, respecting time reversal and crystal symmetries. At high temperatures, Kondo insulators behave as highly correlated metals, while at low temperature they are insulators due to the formation of an energy gap at the Fermi level [14–16]. The opening of a gap at low temperature is attributed to the hybridization between the localized f -electrons and the conduction d -electrons. In SmB_6 , the resistivity increases exponentially as the temperature is decreased, as expected for a normal insulator. However, as the temperature is decreased below 4 K, the resistivity saturates at a finite value (a few Ω cm) [17, 18]. This behavior was attributed to extended states [19], whose nature was revealed recently by transport experiments, identifying them with metallic surface states [6–9] and supporting predictions of the nontrivial topological nature of SmB_6 . ARPES measurements reveal a Kondo gap of ~ 20 meV in the bulk and identify the low-lying bulk in-gap states close to the Fermi level [10–12, 20, 21]. These in-gap states have been associated with magnetic excitations [15, 20, 22] and found to disappear as the temperature is raised above 20–30 K [11, 22]. Other ARPES results suggest that the transition is very broad and that

the in-gap states disappear completely at a much higher temperature [10], or that they gradually transform from 2D to 3D nature with increasing temperature [23, 24].

The magnetic properties of bulk SmB_6 have been extensively studied using magnetization measurements [17], inelastic neutron scattering [22, 25–27], nuclear magnetic resonance (NMR) [28–31] and muon spin relaxation (μ SR) [32]. These measurements detected magnetic excitations at energies below the bulk gap. However, magnetic ordering in the bulk of SmB_6 was ruled out by magnetization [17] and μ SR measurements down to 20 mK [32] (except under high pressure [33]). In contrast, low temperature magnetotransport measurements indicate magnetic ordering at the surface of SmB_6 below 600 mK, which was attributed to ferromagnetic [34] or possibly glassy [35] ordering. This ordering is claimed to involve Sm^{3+} magnetic moments which were detected using x-ray absorption spectroscopy (XAS) at the surface of SmB_6 [36].

Although various theoretical [2–5] and experimental [6–13] studies have now established compelling evidence that SmB_6 is a topological Kondo insulator, a number of open questions remain unanswered. In particular, the source of the magnetic excitations mentioned above is still unclear. It was suggested that an *excitonic state* is responsible for these fluctuations [15, 26, 27, 37]. In this context, it is also important to understand the interplay between these magnetic excitations and the topological surface states in order to elucidate the source of reported magnetic ordering at the surface of SmB_6 [34, 35]. In this paper, we address these important aspects using depth-resolved low-energy μ SR (LE- μ SR) measurements on single-crystal samples of SmB_6 . We detect a clear signature of fluctuating local magnetic fields ap-

pearing below ~ 15 K, similar to our previous bulk measurements [32]. The typical size of the fluctuating field in the bulk is ~ 1.8 mT with a correlation time of ~ 60 ns. Moreover, we find that the magnitude and/or fluctuation time of these magnetic fields decreases gradually near the surface, over a length scale of 40–90 nm, possibly disappearing completely at the surface of SmB_6 . We propose that excitonic states are responsible for these fluctuating magnetic fields. In contrast, we detect an enhancement of static magnetic fields near the surface, which may be attributed to an increasing number of Sm^{3+} moments at the surface of SmB_6 [36].

Experimental details — μSR measurements were performed using the LEM [38, 39] and DOLLY spectrometers at PSI, Switzerland. In these measurements, 100% spin polarized positive muons are implanted into the sample. The evolution of the spin polarization, which depends on the local magnetic fields, is monitored via the anisotropic beta decay positron which is emitted preferentially in the direction of the muon’s spin at the time of decay. Using appropriately positioned detectors one can measure the asymmetry, $A(t)$, of the beta decay along the initial polarization direction. $A(t)$ is proportional to the time evolution of the spin polarization of the ensemble of implanted spin probes [40]. Conventional μSR experiments use surface muons with implantation energy of 4.1 MeV, resulting in a stopping range in typical density solids from 0.1 mm to 1 mm. Thus limiting their application to studies of bulk properties, i.e., they cannot provide depth-resolved information or study extremely thin film samples. Depth-resolved μSR measurement can be performed at the LEM spectrometer using muons with tunable energies in the 1–30 keV range, corresponding to implantation depths of 10–200 nm. All the μSR data reported here were analyzed using the MUSRFIT package [41].

The studied single crystals of SmB_6 samples were grown using the floating-zone method [42]. LE- μSR measurements were performed on a mosaic of 6 disc shaped single crystals, aligned with their [100] axis normal to the surface, and glued on a silver backing plate. The bulk μSR measurements reported here were performed on one of these single crystals.

Results — Figure 1(a) shows typical zero field (ZF) μSR asymmetries, measured at two different temperatures, above and below the “critical” temperature ~ 15 K, i.e., where strong local magnetic field fluctuations appear in bulk SmB_6 [32]. These are compared in Fig. 1(b–d) to LE- μSR measurements at the same temperatures and three different muon implantation energies, E . The corresponding muon stopping profiles in SmB_6 for the different energies, which were calculated using a Monte Carlo program TRIM.SP [43], are shown in Fig. 2. At 20 K we observe a Gaussian-like muon spin damping for all four different energies. This type of damping is attributed to randomly oriented static magnetic fields [40], which reflect the Gaussian field distribution typically produced by dipolar fields from nuclear moments (static on the

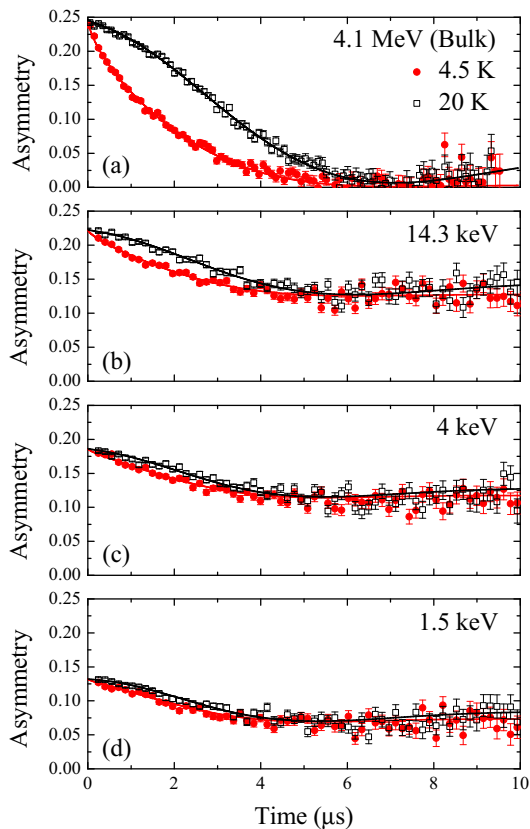


FIG. 1. (Color online) ZF- μSR spectra obtained at different temperatures and implantation energies. The solid lines are fits to Eq. (1).

time scale of μSR). A clear change in the shape of the asymmetry is detected upon cooling (from Gaussian to Lorentzian), which indicates the appearance of additional dilute local magnetic fields and a change in the internal field distribution [44]. Since the dipolar fields from nuclear moments do not change with temperature, we argue that the appearance of additional dilute local magnetic fields is most probably due to electronic magnetic mo-

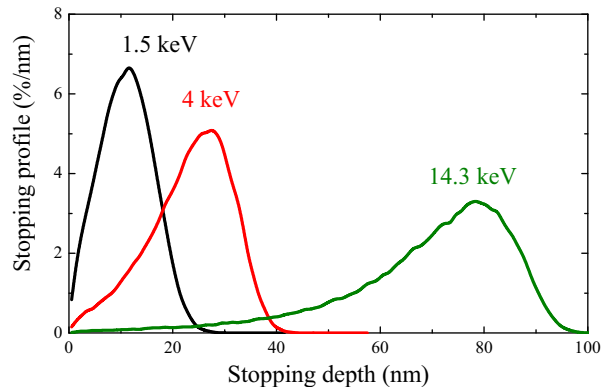


FIG. 2. (Color online) Muon implantation profiles in SmB_6 , calculated using TRIM.SP for various implantation energies.

ments in SmB₆ which are dynamic in nature within the μ SR time scale [32]. Most importantly, however, we find that the difference between the low and high temperature asymmetries becomes less pronounced with decreasing E , i.e., as we approach the surface of the SmB₆. As we discuss below, this indicates that the size and/or fluctuation time of the observed magnetic fields at low temperatures decreases gradually with decreasing depth.

We turn now to a quantitative analysis of our μ SR data. Following the same analysis procedure used previously for the bulk measurements [32], all ZF spectra can be fitted well using a Gaussian Kubo-Toyabe relaxation function multiplied by a stretched exponential decay function,

$$A(t) = A_0 \left\{ \frac{1}{3} + \frac{2}{3} (1 - \sigma^2 t^2) e^{-\frac{\sigma^2 t^2}{2}} \right\} e^{-(\lambda t)^\beta} + A_{\text{bg}}, \quad (1)$$

where A_0 is the initial asymmetry, β is the stretch parameter, and A_{bg} is a non-relaxing background contribution. σ is the width of static field distribution, e.g., due to nuclear moments, while λ is the muon spin relaxation rates due to the presence of dynamic local fields. Note, $A_{\text{bg}} = 0$ in the bulk μ SR measurements, but it is non-zero in the LE- μ SR measurements due to muons missing the sample and landing in the silver backing plate. For consistency with the bulk- μ SR data analysis [32], we

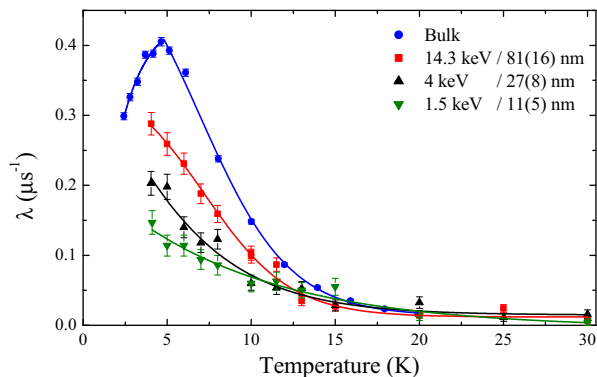


FIG. 3. (Color online) Temperature dependence of the dynamic muon spin relaxation rate λ for different muon implantation energies. The solid lines are guides to the eye.

maintain A_0 , σ and A_{bg} as globally common variables for all temperatures at a particular muon implantation energy. Similarly, we also keep the value obtained from bulk measurements, $\beta = 0.72(1)$, fixed for all temperatures and implantation energies. Figure 3 shows the obtained λ values from the fit as a function of temperature for each implantation energy/depth. We observe a large increase in λ below ~ 15 K in the bulk- μ SR data with a pronounced peak at ~ 4.5 K which we attribute to gradual slowing down in the dynamics of the local magnetic fields at low temperatures [32]. As expected from our qualitative discussion above, we observe similar increase in λ below ~ 15 K for all other implantation

energies, though it becomes less pronounced as we approach the surface. Although a gradual slowing down is observed for all implantation energies, our results clearly show that the nature of magnetic fluctuations strongly depends on depth. In Fig. 4 we plot λ at ~ 4.5 K and σ as a function of the muon implantation depth in SmB₆. The relaxation rate λ decreases rapidly with decreasing depth and may be extrapolated to $\lambda \rightarrow 0$ at the surface of SmB₆ (dashed line). This is accompanied by an increase

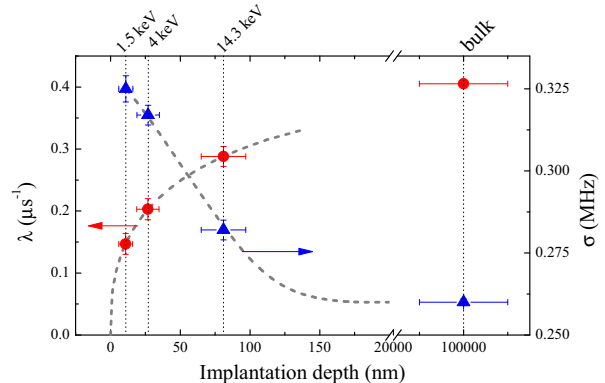


FIG. 4. (Color online) The relaxation rates λ at ~ 4.5 K (red, left axis) and σ (blue, right axis) as a function of muon implantation depth in SmB₆. The dashed lines are guides to the eye and the dotted vertical lines indicate the different E values.

in σ with decreasing depth. The value of σ in the bulk is consistent with what we expect from (predominantly boron) nuclear magnetic moments in this system [32]. Therefore, the observed increase near the surface must be due to additional sources of relatively small and *static* magnetic fields. This may be due to an increased concentration of Sm³⁺ moments near the surface of SmB₆ which was observed in XAS measurements [36]. The increase in σ may hint to a possible magnetic ordering at the surface of SmB₆, such as that reported below 600 mK [34, 35]. However, this cannot be fully confirmed since it is not possible to reach the required low temperatures in LE- μ SR measurements.

Note that λ reflects the spin lattice relaxation rate of the muon spin in ZF, which is proportional to $\Delta B^2 \tau$, where ΔB is the size of the fluctuating local field sensed by the implanted muons and τ is its correlation time. Therefore, the observed decrease in λ at lower implantation energies may be attributed to a decrease in ΔB and/or τ as we approach the surface of SmB₆. To evaluate the size of ΔB and τ we measure the asymmetry as a function of longitudinal magnetic field, i.e., applied along the direction of initial muon spin polarization. The field dependence of λ follows [44–46],

$$\lambda = \frac{2\tau(\gamma\Delta B)^2}{1 + (\tau\gamma B_0)^2}, \quad (2)$$

where $\gamma = 2\pi \times 135.5$ MHz/T is the gyromagnetic ratio of the muon and B_0 is the applied magnetic field. The

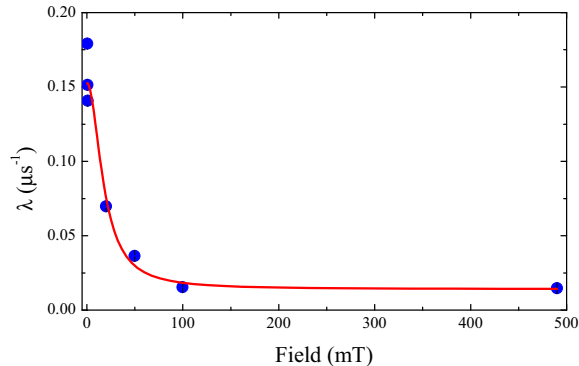


FIG. 5. (Color online) The relaxation rate λ at 1.8 K as a function of applied field [32]. The solid line is the fit described in the text.

experimental results, which were measured in the bulk of SmB_6 at 1.8 K, fit well to Eq. (2) (see Fig. 5) giving $\Delta B = 1.8(2)$ mT and $\tau = 60(10)$ ns [47]. Here we assume that we are in the fast fluctuations limit, $\tau\gamma\Delta B \ll 1$, which is consistent with the values obtained from the fit.

Discussion — We now discuss our data assuming bulk excitons as a source for the observed magnetic fluctuations. The excitons are believed to be of antiferromagnetic nature with a wavelength of the order of a few lattice constants [15, 27]. The observed decay length of magnetic fluctuations near the surface (40–90 nm) should then be interpreted as the coherence length or “size” of the excitons. This size is much larger than the ordering wavelength so that the exciton can be thought of as a fluctuating region with antiferromagnetic correlations.

The measured value $\Delta B \sim 1.8$ mT for the width of the distribution of magnetic fields can be used to estimate the magnitude of the fluctuating magnetic moments. We assume that the muons stop at a random position inside the cubic unit cell of SmB_6 with a lattice constant of 4.13 Å. Calculating the distribution of magnetic fields

due to the antiferromagnetic correlations in the region of the exciton yields an average value of $\sim 0.01\mu_B$ for the magnetic moments, where μ_B is the Bohr magneton.

In addition, we can use a simple hydrogen model for the exciton, describing it as a bound state of an electron and a hole, in order to relate the size to the reduced mass μ_{ex} of the electron–hole pair via $d = a_0\epsilon_r m_e / \mu_{\text{ex}}$. Here, a_0 is the Bohr radius and ϵ_r is the dielectric constant of SmB_6 , which is estimated between $\epsilon_r \sim 600$ [48] and 1500 [49]. Our measurements then imply a reduced mass of the order of the bare electron mass m_e , suggesting that either electrons, holes, or both are relatively light compared to reported values for the effective mass in SmB_6 of $m^* \sim 100 m_e$ [48]. Note that within this model, the observed decrease in λ near the surface is primarily due to the absence of excitonic states and associated magnetic fields in this region.

Conclusions — In conclusion, we observe fluctuating magnetic fields appearing only below ~ 15 K in the bulk of SmB_6 . Using LE- μ SR measurements we find that these fields are rapidly suppressed with decreasing depth and probably disappear completely at the surface. We attribute these fluctuating fields to excitonic states, whose extent is limited to the bulk of SmB_6 and disappears within ~ 60 nm of its surface. An estimate of $\sim 0.01\mu_B$ for the average magnitude of magnetic moments is obtained from the distribution of fluctuating magnetic fields. We also observe a slight increase in the distribution width of static magnetic fields near the surface of SmB_6 , hinting to the appearance of additional magnetic moments in this region. Our results reveal a complex magnetic behavior near the surface of the 3D topological Kondo insulator SmB_6 . We expect that the magnetic nature of the near surface region of SmB_6 may have significant implications on the topological surface states at very low temperatures.

This work was performed at the Swiss Muon Source ($S\mu S$), Paul Scherrer Institute (PSI, Switzerland). The work was supported, in part, by the EPSRC, United Kingdom grant no. EP/I007210/1.

* pabitra.biswas@stfc.ac.uk

† zaher.salman@psi.ch

- [1] J. E. Moore, *Nature* **464**, 194 (2010).
- [2] M. Dzero, K. Sun, V. Galitski, and P. Coleman, *Phys. Rev. Lett.* **104**, 106408 (2010).
- [3] V. Alexandrov, M. Dzero, and P. Coleman, *Phys. Rev. Lett.* **111**, 226403 (2013).
- [4] F. Lu, J. Z. Zhao, H. Weng, Z. Fang, and X. Dai, *Phys. Rev. Lett.* **110**, 096401 (2013).
- [5] M. Dzero, K. Sun, P. Coleman, and V. Galitski, *Phys. Rev. B* **85**, 045130 (2012).
- [6] S. Wolgast, Ç. Kurdak, K. Sun, J. W. Allen, D.-J. Kim, and Z. Fisk, *Phys. Rev. B* **88**, 180405 (2013).
- [7] D. J. Kim, S. Thomas, T. Grant, J. Botimer, Z. Fisk, and J. Xia, *Scientific Reports* **3**, 3150 (2013).
- [8] X. Zhang, N. P. Butch, P. Syers, S. Ziemak, R. L. Greene, and J. Paglione, *Phys. Rev. X* **3**, 011011 (2013).
- [9] D. J. Kim, J. Xia, and Z. Fisk, *Nat Mater* **13**, 466 (2014).
- [10] N. Xu, X. Shi, P. K. Biswas, C. E. Matt, R. S. Dhaka, Y. Huang, N. C. Plumb, M. Radović, J. H. Dil, E. Pomjakushina, K. Conder, A. Amato, Z. Salman, D. M. Paul, J. Mesot, H. Ding, and M. Shi, *Phys. Rev. B* **88**, 121102 (2013).
- [11] M. Neupane, N. Alidoust, S.-Y. Xu, T. Kondo, Y. Ishida, D. J. Kim, C. Liu, I. Belopolski, Y. J. Jo, T.-R. Chang, H.-T. Jeng, T. Durakiewicz, L. Balicas, H. Lin, A. Bansil, S. Shin, Z. Fisk, and M. Z. Hasan, *Nat. Commun.* **4**, 2991 (2013).
- [12] J. Jiang, S. Li, T. Zhang, Z. Sun, F. Chen, Z. R. Ye, M. Xu, Q. Q. Ge, S. Y. Tan, X. H. Niu, M. Xia, B. P. Xie, Y. F. Li, X. H. Chen, H. H. Wen, and D. L. Feng, *Nat. Commun.* **4**, 3010 (2013).

- [13] N. Xu, P. K. Biswas, J. H. Dil, R. S. Dhaka, G. Landolt, S. Muff, C. E. Matt, X. Shi, N. C. Plumb, M. Radović, E. Pomjakushina, K. Conder, A. Amato, S. V. Borisenko, R. Yu, H.-M. Weng, Z. Fang, X. Dai, J. Mesot, H. Ding, and M. Shi, *Nat. Commun.* **5**, 4566 (2014).
- [14] G. Aeppli and Z. Fisk, *Comments Condens. Matter Phys.* **16**, 155 (1992).
- [15] P. S. Riseborough, *Annalen der Physik* **9**, 813 (2000).
- [16] P. Coleman, *Heavy Fermions: electrons at the edge of magnetism* (Wiley Online Library, 2007).
- [17] A. Menth, E. Buehler, and T. H. Geballe, *Phys. Rev. Lett.* **22**, 295 (1969).
- [18] J. W. Allen, B. Batlogg, and P. Wachter, *Phys. Rev. B* **20**, 4807 (1979).
- [19] J. C. Cooley, M. C. Aronson, Z. Fisk, and P. C. Canfield, *Phys. Rev. Lett.* **74**, 1629 (1995).
- [20] H. Miyazaki, T. Hajiri, T. Ito, S. Kunii, and S.-I. Kimura, *Phys. Rev. B* **86**, 075105 (2012).
- [21] J. D. Denlinger, G. H. Gweon, J. W. Allen, C. G. Olson, Y. Dalichaouch, B. W. Lee, M. B. Maple, Z. Fisk, P. C. Canfield, and P. E. Armstrong, *Physica B: Condensed Matter* **281-282**, 716 (2000).
- [22] P. Alekseev, J.-M. Mignot, J. Rossat-Mignod, V. Lazukov, and I. Sadikov, *Physica B: Condensed Matter* **186-188**, 384 (1993).
- [23] J. D. Denlinger, J. W. Allen, J.-S. Kang, K. Sun, B.-I. Min, D.-J. Kim, and Z. Fisk, *JPS Conf. Proc.* **3**, 017038 (2014).
- [24] J. D. Denlinger, J. W. Allen, J.-S. Kang, K. Sun, J.-W. Kim, J. H. Shim, B. I. Min, D.-J. Kim, and Z. Fisk, *arXiv:1312.6637*.
- [25] P. A. Alekseev, J. M. Mignot, J. Rossat-Mignod, V. N. Lazukov, I. P. Sadikov, E. S. Konovalova, and Y. B. Paderno, *J. Phys.: Condens. Matter* **7**, 289 (1995).
- [26] P. A. Alekseev, V. N. Lazukov, K. S. Nemkovskii, and I. P. Sadikov, *J. Exp. Theor. Phys.* **111**, 285 (2010).
- [27] W. T. Fuhrman, J. Leiner, P. Nikolić, G. E. Granroth, M. B. Stone, M. D. Lumsden, L. DeBeer-Schmitt, P. A. Alekseev, J.-M. Mignot, S. M. Koohpayeh, P. Cottingham, W. A. Phelan, L. Schoop, T. M. McQueen, and C. Broholm, *Phys. Rev. Lett.* **114**, 036401 (2015).
- [28] M. Takigawa, H. Yasuoka, Y. Kitaoka, T. Tanaka, H. Nozaki, and Y. Ishizawa, *Journal of the Physical Society of Japan* **50**, 2525 (1981).
- [29] T. Caldwell, *Nuclear Magnetic Resonance Studies of Field Effects on Single Crystal SmB₆*, Ph.D. thesis, The Florida State University (2004).
- [30] T. Caldwell, A. P. Reyes, W. G. Moulton, P. L. Kuhns, M. J. R. Hoch, P. Schlottmann, and Z. Fisk, *Phys. Rev. B* **75**, 075106 (2007).
- [31] P. Schlottmann, *Phys. Rev. B* **90**, 165127 (2014).
- [32] P. K. Biswas, Z. Salman, T. Neupert, E. Morenzoni, E. Pomjakushina, F. von Rohr, K. Conder, G. Balakrishnan, M. C. Hatnean, M. R. Lees, D. M. Paul, A. Schilling, C. Baines, H. Luetkens, R. Khasanov, and A. Amato, *Phys. Rev. B* **89**, 161107 (2014).
- [33] A. Barla, J. Derr, J. P. Sanchez, B. Salce, G. Laperot, B. P. Doyle, R. Rüffer, R. Lengsdorf, M. M. Abd-Elmeguid, and J. Flouquet, *Phys. Rev. Lett.* **94**, 166401 (2005).
- [34] Y. Nakajima, P. Syers, X. Wang, R. Wang, and J. Paglione, *Nat. Phys.* **12**, 213 (2016).
- [35] S. Wolgast, Y. S. Eo, T. Öztürk, G. Li, Z. Xiang, C. Tinsman, T. Asaba, B. Lawson, F. Yu, J. W. Allen, K. Sun, L. Li, Ç. Kurdak, D.-J. Kim, and Z. Fisk, *Phys. Rev. B* **92**, 115110 (2015).
- [36] W. A. Phelan, S. M. Koohpayeh, P. Cottingham, J. W. Freeland, J. C. Leiner, C. L. Broholm, and T. M. McQueen, *Phys. Rev. X* **4**, 031012 (2014).
- [37] J. Knolle and N. R. Cooper, *arXiv:1608.02453*.
- [38] E. Morenzoni, F. Kottmann, D. Maden, B. Matthias, M. Meyberg, T. Prokscha, T. Wutzke, and U. Zimmermann, *Phys. Rev. Lett.* **72**, 2793 (1994).
- [39] T. Prokscha, E. Morenzoni, K. Deiters, F. Foroughi, D. George, R. Kobler, A. Suter, and V. Vrankovic, *Nuc. Inst. Phys. A* **595**, 317 (2008).
- [40] A. Yaouanc and P. D. d. Réotier, *Muon Spin Rotation, Relaxation, and Resonance: Applications to Condensed Matter* (OUP Oxford, 2010).
- [41] A. Suter and B. Wojek, *Physics Procedia* **30**, 69 (2012).
- [42] M. Ciomaga Hatnean, M. R. Lees, D. McK. Paul, and G. Balakrishnan, *Scientific Reports* **3**, 3071 (2013).
- [43] E. Morenzoni, H. Glückler, T. Prokscha, R. Khasanov, H. Luetkens, M. Birke, E. M. Forgan, C. Niedermayer, and M. Pleines, *Nuclear Instruments and Methods in Physics Research Section B* **192**, 254 (2002).
- [44] Y. J. Uemura, T. Yamazaki, D. R. Harshman, M. Senba, and E. J. Ansaldo, *Phys. Rev. B* **31**, 546 (1985).
- [45] A. Keren, *Phys. Rev. B* **50**, 10039 (1994).
- [46] Z. Salman, A. Keren, P. Mendels, V. Marvaud, A. Sculler, M. Verdaguer, J. S. Lord, and C. Baines, *Phys. Rev. B* **65**, 132403 (2002).
- [47] The contribution from the level crossing seen at high temperature is subtracted before fitting the data. An additional field independent offset is also needed to fit the data, which we attribute to other possible sources of relaxation.
- [48] B. Gorshunov, N. Sluchanko, A. Volkov, M. Dressel, G. Knebel, A. Loidl, and S. Kunii, *Phys. Rev. B* **59**, 1808 (1999).
- [49] G. Travaglini and P. Wachter, *Phys. Rev. B* **29**, 893 (1984).